LBL-33660
UC-200

Lawrence Berkeley Laboratory
UNIVERSITY OF CALIFORNIA

EARTH SCIENCES DIVISION

Presented at the International High Level Radioactive
Waste Management Conference, Las Vegas, NV,
April 26–30, 1993, and to be published in the Proceedings

Single Fracture Aperture Patterns: Characterization by Slit-Island Fractal Analysis

B.L. Cox and J.S.Y. Wang

January 1993

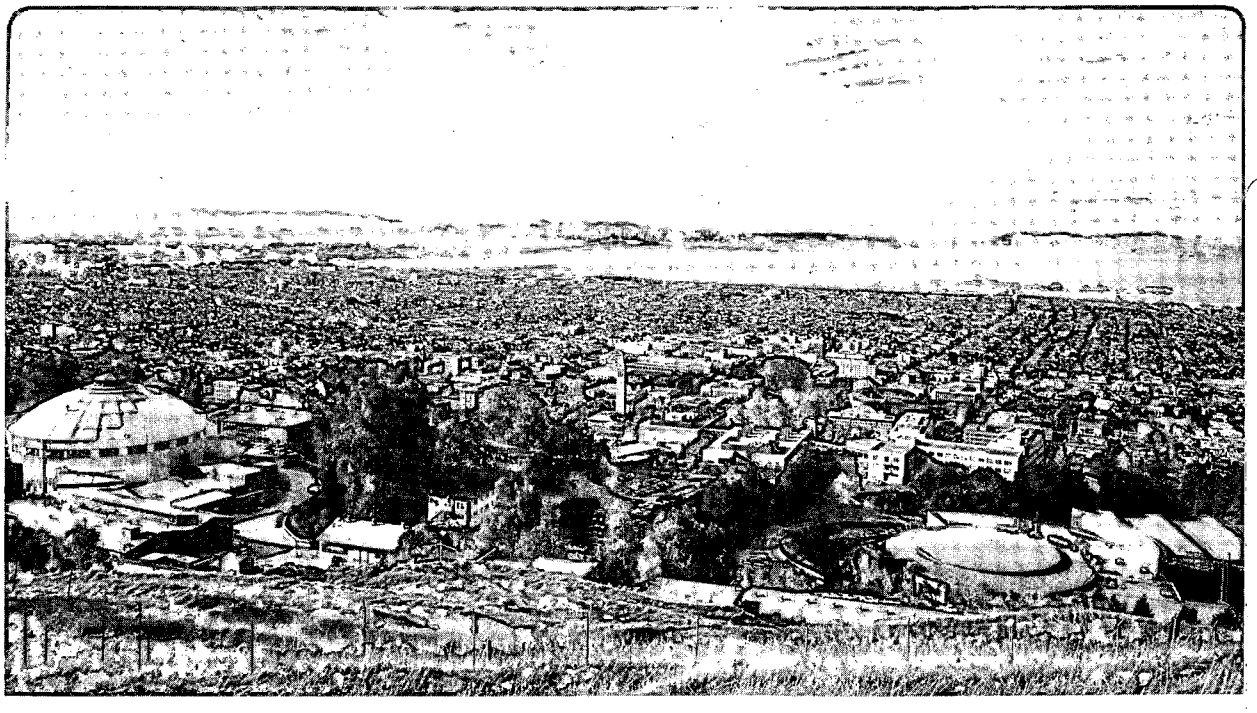

LOAN COPY
Circulates
for 4 weeks
Bldg. 50 Library.
Copy 2
LBL-33660

Prepared for the U.S. Department of Energy under Contract Number DE-AC03-76SF00098

DISCLAIMER

This document was prepared as an account of work sponsored by the United States Government. Neither the United States Government nor any agency thereof, nor The Regents of the University of California, nor any of their employees, makes any warranty, express or implied, or assumes any legal liability or responsibility for the accuracy, completeness, or usefulness of any information, apparatus, product, or process disclosed, or represents that its use would not infringe privately owned rights. Reference herein to any specific commercial product, process, or service by its trade name, trademark, manufacturer, or otherwise, does not necessarily constitute or imply its endorsement, recommendation, or favoring by the United States Government or any agency thereof, or The Regents of the University of California. The views and opinions of authors expressed herein do not necessarily state or reflect those of the United States Government or any agency thereof or The Regents of the University of California and shall not be used for advertising or product endorsement purposes.

Lawrence Berkeley Laboratory is an equal opportunity employer.

This publication has been reproduced from the best available copy

DISCLAIMER

This document was prepared as an account of work sponsored by the United States Government. While this document is believed to contain correct information, neither the United States Government nor any agency thereof, nor the Regents of the University of California, nor any of their employees, makes any warranty, express or implied, or assumes any legal responsibility for the accuracy, completeness, or usefulness of any information, apparatus, product, or process disclosed, or represents that its use would not infringe privately owned rights. Reference herein to any specific commercial product, process, or service by its trade name, trademark, manufacturer, or otherwise, does not necessarily constitute or imply its endorsement, recommendation, or favoring by the United States Government or any agency thereof, or the Regents of the University of California. The views and opinions of authors expressed herein do not necessarily state or reflect those of the United States Government or any agency thereof or the Regents of the University of California.

LBL-33660

Single Fracture Aperture Patterns: Characterization by Slit-Island Fractal Analysis

B. L. Cox and J. S. Y. Wang

Earth Sciences Division
Lawrence Berkeley Laboratory
University of California
Berkeley, California 94720

January 1993

This work was supported by the Director, Office of Civilian Radioactive Waste Management, Yucca Mountain Site Characterization Project Office, Regulatory and Site Evaluation Division, under U.S. Department of Energy Contract No. DE-AC03-76SF00098.

Printed on recycled paper

SINGLE FRACTURE APERTURE PATTERNS: CHARACTERIZATION BY SLIT-ISLAND FRACTAL ANALYSIS

B. L. Cox and J. S. Y. Wang
Earth Sciences Division, Lawrence Berkeley Laboratory
Berkeley, California 94720
(510) 486-4717

ABSTRACT

Fracture aperture surfaces from two different fractures (one crack and one fault) are characterized and compared using geostatistical and fractal methods. Slit-island fractal dimensions of 1.3 and 1.4 are very similar. Cutoff patterns ("indicator maps") are not similar: the crack has a radial pattern and the fault has elongated patterns in the faulting direction. The cutoff patterns could be used to test the significance of these two different patterns for single fracture fluid flow models.

I. INTRODUCTION

Single fracture measurements are difficult to obtain, but they are the only means we have to observe and study natural fracture morphology. The character of the fracture openings (apertures) is often one of the primary factors controlling fluid flow in the fracture. In particular, the shape, distribution, and connectivity of contact areas and flow channels can affect the relative permeability of wetting and non-wetting fluid phases in unsaturated systems. In this paper we use three methods of fractal analysis (the slit-island, the divider, and the variogram) as well as statistical and geostatistical analysis to characterize the geometry of measured fracture apertures obtained from two different fractured rock specimens from the field. One of these is a granitic fracture (crack) of homogeneous lithology and no displacement; the other is a fracture (fault) obtained from a highly altered fault zone, containing striations and slickensides. We discuss the fractal and geostatistical analysis of these two fractures in the context of what information is most helpful for making predictions about fluid flow in single fractures.

II. FRACTURE APERTURE DATA

Fracture aperture measurements of a faulted rock fracture from Dixie Valley, Nevada, were obtained by three different (and non-destructive) fracture measurement techniques. The fracture aperture patterns were measured by profilometry,[1] by light transmission through translucent silicone casts,[2] and by light transmission through dyed fluid in epoxy replicas of the rock.[3] For this paper, we examine Dixie Valley fracture apertures measured by the dyed fluid method[3] and compare this aperture topography with that of a second fracture obtained from a Stripa granite[4] measured by the same technique. We could use the same techniques to compare the variability of the three Dixie Valley data sets measured by different techniques, in order to distinguish intrinsic features from experimental artifacts.

III. STATISTICS AND GEOSTATISTICS ANALYSES

The aperture data measured by the dyed fluid technique[3,4] for the Stripa and Dixie Valley fractures are displayed on surface plots and histograms in Figure 1. The Stripa fracture shown is a 403 by 403 pixel array, while the Dixie Valley fracture is a 369 by 369 pixel array. Both have between-pixel spacings of approximately 0.2 μm, so the Stripa surface is approximately 81 mm on a side, and the Dixie Valley surface is around 74 mm on a side. The histograms of the two apertures both show sharp peaks at large apertures, at 160 μm for the Stripa fracture, and at 240 μm for the Dixie Valley fracture. These peaks have been attributed to experimental artifact in which, for a particular dye, there is a maximum aperture above which the method cannot distinguish variation. Representative profiles (row 150) through both fractures are shown in Figure 2 and for both of these, the extreme values occur as part of local topographic highs. We calculated the statistics (shown in Figure 1) with and without this population of largest but unknown apertures. After removing the extreme values, the mean and standard deviation of the Stripa fracture are 37 μm and 21 μm, and those of the Dixie Valley fracture are 42 μm and 21 μm. The skewness for the Dixie Valley fracture is more positive than for the Stripa fracture, indicating that more elevations fall below the mean for the Dixie Valley fracture. The kurtosis for Dixie Valley indicates a more peaked distribution than that of the Stripa fracture.

The variograms in the row (x) and column (y) directions for the two fractures are displayed on Figure 3. The variable plotted on the y-axis is the semi-variance, v, where

$$v(h) = \frac{1}{2n} \sum_{i=1}^{i=n(h)} (z(x_i) - z(x_i + h))^2$$

This summation was made for all the rows, and the average was computed for each sample distance point (h). The same procedure was then repeated for the columns (the y-direction). These variograms have not been pre-processed to remove trends, except that sample points with extreme values were not included in these variogram calculations. The correlation length of the two fractures (by visual estimation) is approximately 150 grid points (30 μm) for the Stripa fracture row variogram and 100 grid points (20 μm) for the Dixie Valley fracture row variogram. The visual estimation was obtained by looking at the variogram, and estimating the spacing at which the first sill is reached.

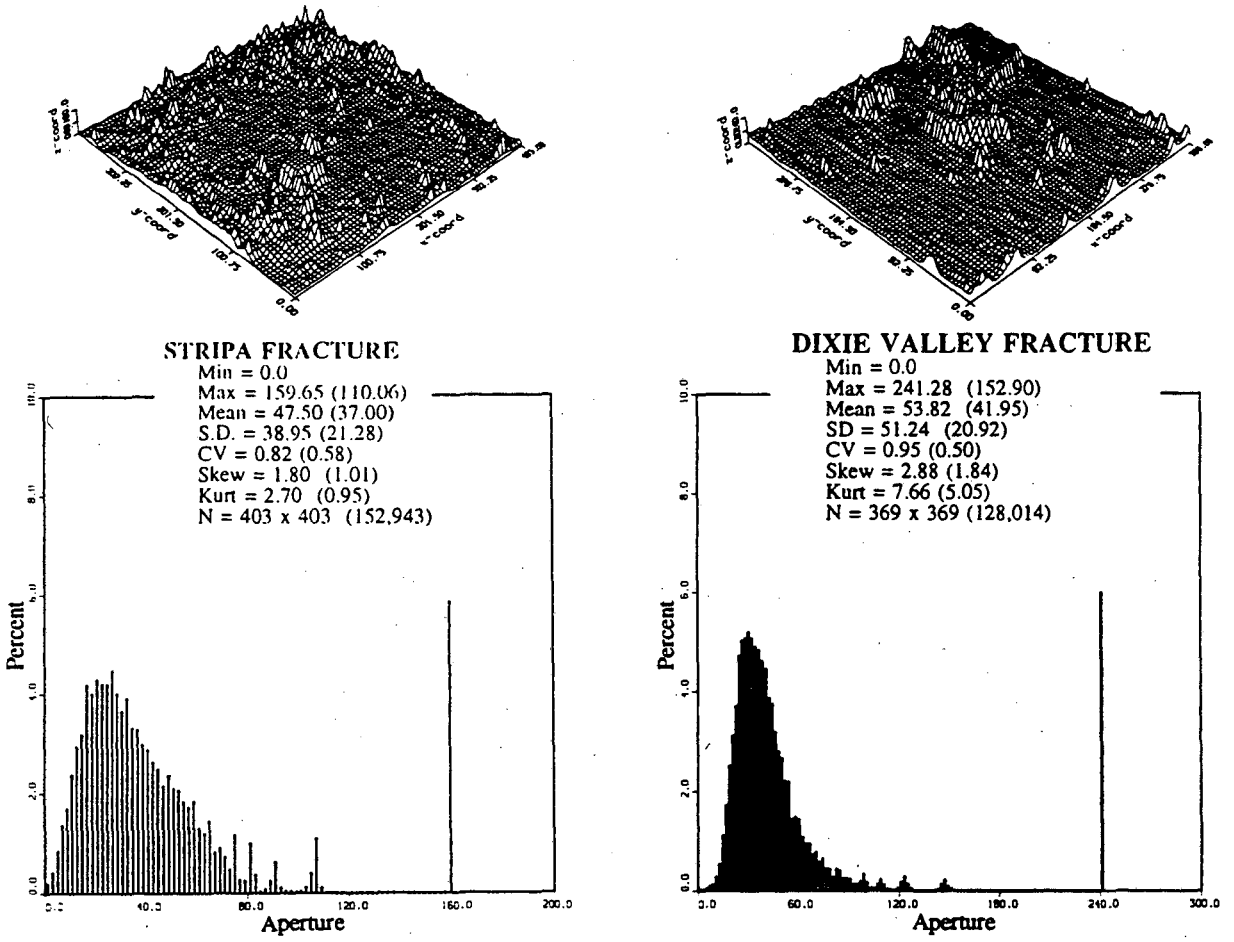

Figure 1. Surface plots and histograms for Stripa (a) and Dixie Valley (b) fractures. Values in parentheses are statistics with the extreme values removed.

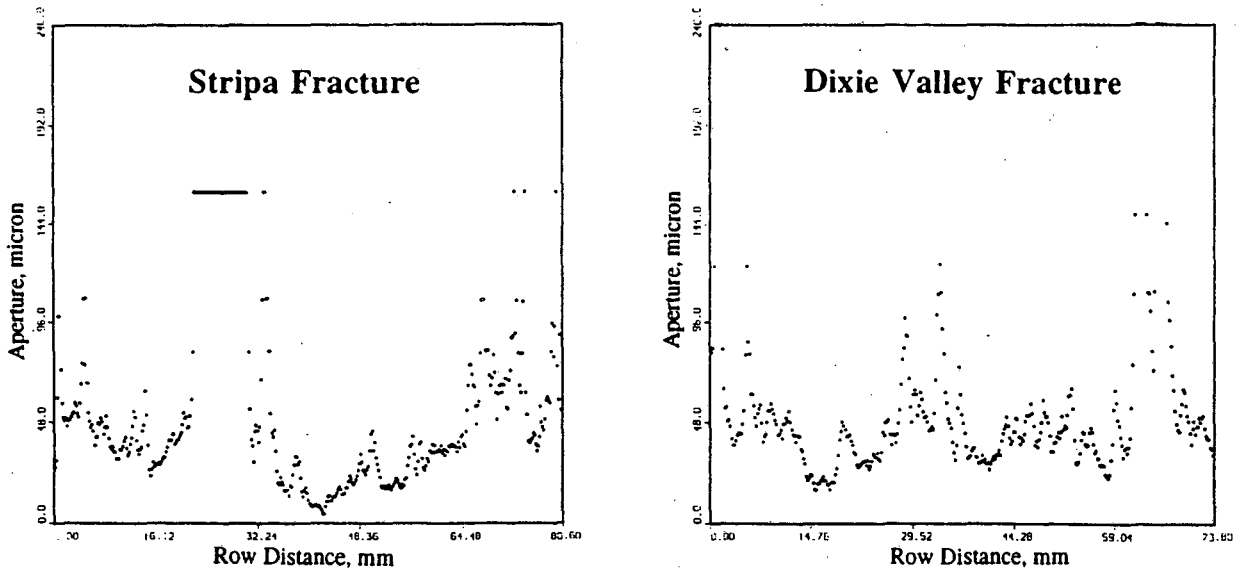

Figure 2. Profiles taken along row 150 for the Stripa (a) and Dixie Valley (b) fractures.

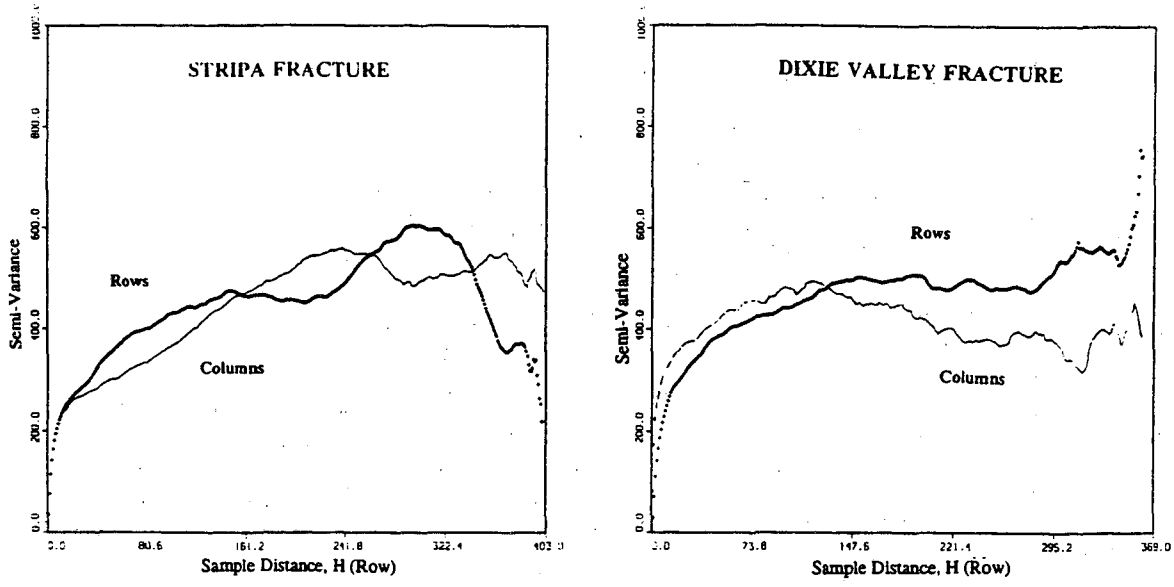

Figure 3. Variograms (in row and column directions) for Stripa (a) and Dixie Valley (b) fractures.

IV. FRACTAL ANALYSES

Fractal geometry offers an approach to geometric description of irregular geometric patterns.[5] The fractal dimension of topographic surfaces measures the rate of change in the total length of contours or profiles as a function of the rate of change of a measurement interval. The fractal analysis of surfaces can be approached by at least 7 different measurement methods,[6] including the divider, variogram, and slit-island methods.

A. Divider and Variogram Methods

Profiles and variograms may be analyzed to determine a fractal dimension of topographic surfaces.[7] However, this analysis is one-dimensional, in contrast to the slit-island technique, which is two-dimensional. The slope of the log-log plot of the profile length versus the sampling (ruler or divider) length is used to determine the fractal dimension by the relationship D_p=2−slope , where the profile length is the total length of the profile calculated along the sampling length (ruler length) intervals. The variogram fractal dimension is determined by plotting the semivariance versus the sampling distance on a log-log plot, and using the relationship D_v=(4−slope)/2. The profile and variogram fractal dimensions are not equivalent. Log-log plots containing both variograms (the increasing function) and profile lengths (decreasing function) as a function of sampling distance, are shown in Figure 4. For our analyses we determined the frac-

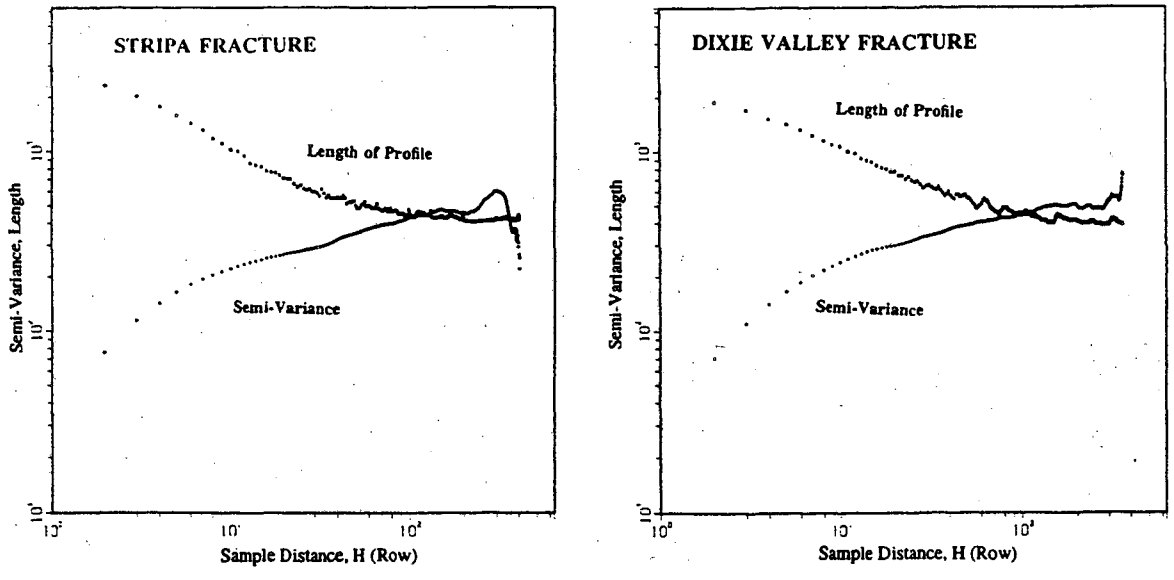

Figure 4. Profile lengths and variograms in the row direction for Stripa (a) and Dixie Valley (b) fractures.

Table 1. Profile and Variogram Fractal Analysis

Name	Orient	No.	P Slope[1]	V Slope[2]	Dp[3]	Dv[4]
Stripa	Rows	200	-0.31	0.32	1.31	1.84
Stripa	Rows	100	-0.41	0.38	1.41	1.81
Stripa	Cols	200	-0.33	0.31	1.33	1.84
Stripa	Cols	100	-0.40	0.27	1.40	1.86
DixVal	Rows	150	-0.35	0.35	1.35	1.82
DixVal	Rows	100	-0.38	0.39	1.38	1.80
DixVal	Cols	150	-0.44	0.21	1.44	1.90
DixVal	Cols	100	-0.49	0.24	1.49	1.88

[1] P slope is the slope of the profile length from H=2 to H=maxH grid spacings (see Figure 4).

[2] V slope is the slope of the variogram (see Figure 4) from H=1 to H=max H grid spacings.

[3] Dp and Dv are the fractal dimensions from the profile length and viogram slopes, respectively.

tal dimension over different ranges of sample distances in the row (x) and column (y) directions, shown in Table 1. The fractal dimension for the profiles sampled up to 200 grid points separation in the row direction were 1.3 and 1.4 for the Stripa and Dixie Valley fractures, respectively. If a shorter sampling distance was analyzed, the Stripa fractal dimension was 1.4 and the Dixie Valley fractal dimension was also 1.4. The Stripa profile fractal dimensions were the same in the column and row directions, if the same sampling distance was chosen. The Dixie Valley profile fractal dimensions were higher in the column direction. The slopes of the Stripa fracture were less sensitive to the direction of the profiles than those of the Dixie Valley fracture.

The variogram fractal dimensions averaged 1.8 for both the Stripa and Dixie Valley fractures. The Dixie Valley fractal dimensions were higher in the column directions. The variogram slopes for the Dixie Valley fracture were very sensitive to direction.

B. Slit-Island Method

The slit-island method was first introduced by Mandelbrot et al.[8] who used it to determine the fractal dimension of steel fractures. They filled steel fracture faces with nickel, then polished the fracture faces parallel to the fracture plane, so that approximately equal amounts of nickel and steel were evident on the polished fracture faces. This created a pattern of islands of nickel in a sea of steel, which they called "slit-islands." We applied this technique numerically to topographic surfaces of data measurements (aperture thickness) by selecting several cutoffs, creating surface contours which divide the surface into two kinds of shapes, positive (islands) and negative (water). There is a range of sizes of these shapes, and the entire collection of either positive or negative shapes is treated as a population. Both the perimeter and area are measured for each island, and the measurements are plotted on a log-log plot, with the perimeter on the x-axis and the area on the y-axis. If the measurements fall on a straight line, this implies a self-similarity to the scaling of the population, and the slope can be used to determine the fractal dimension D where D=2/slope. The pattern of the contours becomes more eroded and permeable with higher fractal dimension, so that the area grows more slowly than the perimeter.

The log-log plots of the cutoffs of the two fractures all fell on straight lines with least squares correlation coefficients of greater than 0.9. Figure 5 shows the perimeter versus area plots for the 50 μm cutoffs. Three cutoffs for each fracture are displayed in Figure 6, where the white areas represent aperture openings larger than the cutoffs, and the dark areas apertures smaller than the cutoffs. (These cutoffs are referred to as "indicator maps" in the geostatistics literature.[9]) The result of the

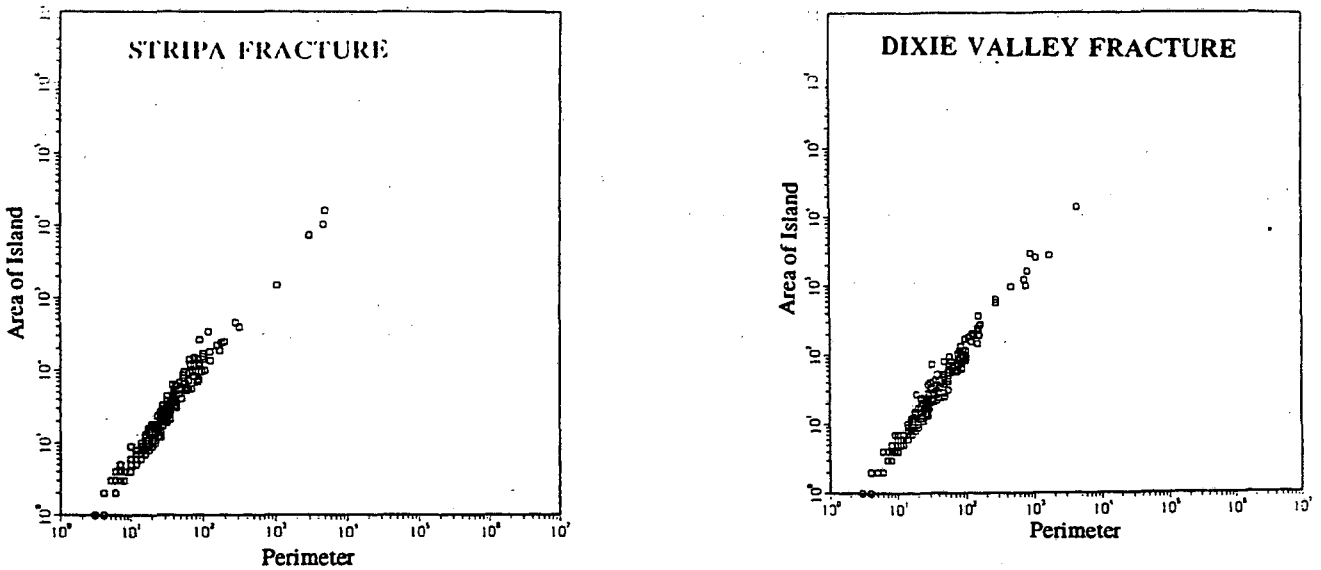

Figure 5. Slit-island analysis for Stripa (a) and Dixie Valley (b) fractures for the 50 micron cutoff.

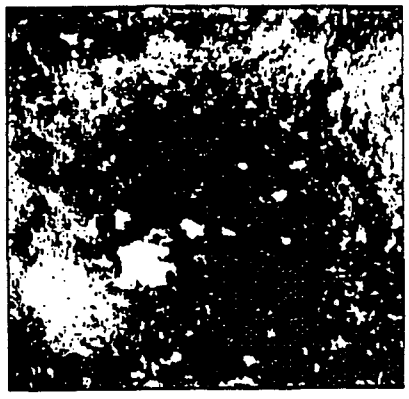

Stripa Fracture: > 50 microns white

Dixie Valley Fracture: > 50 microns white

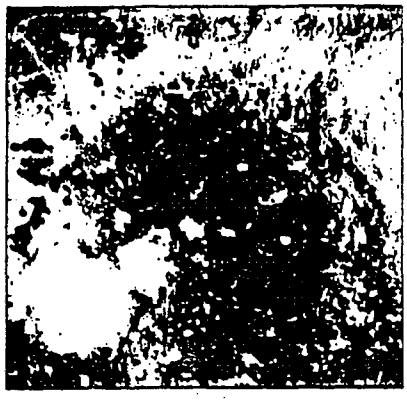

Stripa Fracture: > 37 microns white

Dixie Valley Fracture: > 40 microns white

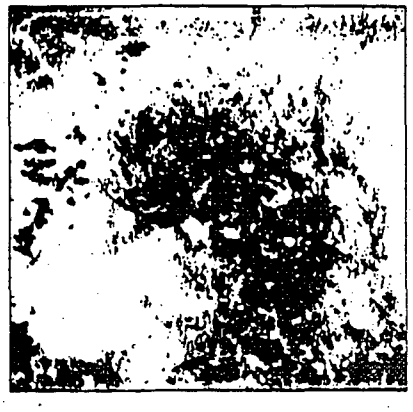

Stripa Fracture: > 27 microns white

Dixie Valley Fracture: > 30 microns white

Figure 6. Cutoffs (indicator maps) for Stripa and Dixie Valley fractures.

Table 2. Slit Island Analyses

Name	Cutoff[1]	No. Is.[2]	Area %[3]	Total Perimeter[4]	Slope[5]	Ds[6]
Stripa	27.	536	36	25890	1.52	1.31
Stripa	37.	791	55	27790	1.54	1.30
Stripa	50.	919	72	26470	1.51	1.33
Stripa	(37.)	(653)	(45)	(27790)	(1.49)	(1.34)
Dix Val	30.	383	28	29970	1.44	1.39
Dix Val	40.	698	53	33280	1.43	1.40
Dix Val	50.	897	71	26040	1.47	1.36
Dix Val	(40.)	(598)	(47)	(33280)	(1.44)	(1.39)

[1] Cutoff is in micrometers.

[2] No. Is. are islands greater than cutoffs (except for those in parentheses).

[3] Percent area is area with apertures greater than cutoff.

[4] Total perimeter is in grid units (grid spacing approximately .2 micrometers).

[5] Slope is from log-log area versus perimeter plots (e.g. Figure 5).

[6] Ds is the fractal dimension from the slit-island slope.

Cutoffs in parentheses are for the inverses analysis (i.e. islands are aperutres less than the cutoff).

fractal analysis for each cutoff is shown in Table 2. The fractal dimension of the Stripa fracture is around 1.3, while that of the Dixie Valley fracture is around 1.4, with ranges of only 0.04 for the different cutoffs. Different cutoffs gave consistently similar fractal dimensions, and when inverted analyses were done, using the areas of the "water" instead of the "islands," the same fractal dimensions were obtained. (These appear in Table 2 in parentheses). The number of islands, the percent area of the islands, and the total perimeter are shown for each cutoff in Table 2. The maximum perimeter occurs at the cutoff closest to the median cutoff. The maximum perimeter for the Dixie Valley fracture is greater than that of the Stripa fracture.

V. DISCUSSION

A. Comparison of Fractal Measurement Techniques

There are potential problems with all fractal measurement techniques[6] including the slit-island technique. Different techniques do not always give the same fractal dimension, and there may even be variability within a single technique, depending on how it is applied to the data. The slit-island and profile fractal analyses were very close for the two fractures. However, the variogram fractal analyses were different. The review of fractal measurement techniques[6] indicated that the variogram fractal dimensions seem to be consistently higher than those of other techniques. Our use of the variogram formula to our data confirmed this earlier observation. There is more variability in the one-dimensional profile and variogram methods, depending on the length of the sample spacing, and depending on direction, than is seen for the slit-island method for different cutoffs. The variability in the two directions indicates some anisotropy, and the need to correct for self-affine scaling. However, all three fractal analyses show that the fractal dimensions of the two fractures are very similar to each other, with a slightly higher fractal dimension for the Dixie Valley fracture. The total perimeter of the Dixie Valley fracture for the intermediate cutoff is also higher, indicating that the total boundary contact between the fluid and the rock is higher for the Dixie Valley fracture. This might imply more resistance to fluid flow along the contacts.

B. Use of Fracture Aperture Data for Modeling

Both the fractal analyses and the statistics of the two fractures show that they have similar means, standard deviations, and fractal dimensions. The variograms show that there is evident anisotropy in the Dixie Valley fracture. However, the cutoff patterns for the two fractures look very different (Figure 6). The Stripa fracture shows a somewhat radial pattern of shapes, while the Dixie Valley fracture shows shapes which are extended in the sliding direction. These two very different patterns might have very different consequences for fluid flow. We could test the hypothesis that these patterns have significantly different effects on fluid flow by both numerical and physical experiments.

The concept of a cutoff pattern can be applied to aperture distributions to determine the possibility of different phase occupancy.[2,10] Starting with a discretized description of fracture aperture, the lowest cutoff can be chosen to represent an expected contact area. Then a "local parallel-plate approximation" can be made to determine the phase occupancy of different fracture aperture segments, and to calculate their permeability. At some given capillary suction pressure P_c, all fracture segments with apertures less than some critical cutoff $z<z_c$ (but greater than the solid phase cutoff) are assumed to allow occupation by water

(wetting phase), while all apertures greater than the critical cutoff $z>z_c$ are assumed to be accessible to air (non-wetting phase). The corresponding wetting phase saturation can be calculated by directly summing over the fracture segments with $z<z_c$ and dividing by the total fracture void volume. After phase occupancy for a given capillary suction has been determined, effective permeability to wetting and non-wetting phases can be calculated by applying a suitable pressure drop across the fracture, and simulating steady single-phase flow in the network of occupied fracture segments.[2,10]

A coarse average of a region of one of the fracture aperture distributions for the Dixie Valley rock specimen was previously analyzed for relative permeability by the method just described.[2] The analysis suggested that in small fractures with numerous asperity contacts contiguous liquid flow paths exist even at small values of liquid saturation with strong capillary suction conditions. The cutoff patterns we display in Figure 6 show the variation in pattern with different cutoffs. For a single phase fluid, one could visually estimate the continuity of the fluid phase for different cutoffs, where the cutoffs could represent the degree of fracture opening. At some maximum opening the parallel plate model for fracture permeability might be adequate, while at some tighter average aperture, the pattern of the openings would become important.

Cutoff patterns for 3 phases for the two fractures are shown in Figure 7. Here, the darkest region is the solid rock phase, the grey area is water (small apertures), and the white areas are air (large apertures). For this set of cutoffs, it appears that the water and air phases together are continuous for the Dixie Valley fracture. However, the pattern in the Stripa fracture has a radial pattern, and seems to visually offer more resistance to fluid flow in the north-south direction and possibly less resistance in the east-west direction. These types of patterns could be used to test models (both computer and laboratory) for faulted versus radial patterns. If variability in the geometry of these otherwise similar fracture patterns does not result in a very different fluid flow regime, then a stochastic model such as Figure 8, or even a simpler model might be adequate.

VI. CONCLUSIONS

1. The fractal dimensions, means, and standard deviations for the Stripa and Dixie Valley apertures, measured with the dyed fluid technique were very similar. The slit-island and profile fractal dimensions were practically identical, while the variogram fractal dimension was much higher. High variogram fractal dimensions were also observed in a literature review of fractal surface measurement techniques.[6]

2. The cutoff patterns were distinctly different, and were not similar to typical stochastic patterns such as Figure 8. The Stripa cutoff patterns showed a radial pattern, while the Dixie Valley cutoff patterns showed patterns elongated in the sliding direction.

3. The cutoff patterns (or "indicator maps") could be used in flow models[2,10] to determine if the pattern would make a difference in the fluid flow characteristics. These predictions could then be tested by comparing flow visualization laboratory experiments in the two different fracture replicas.[3]

4. The slit-island fractal analysis indicates a higher fractal dimension and a higher total perimeter for the Dixie Valley fracture. In the absence of information about anisotropy or connectedness, the higher fractal dimension might indicate greater resistance to flow. However, visual inspection of the cutoff patterns suggests that the anisotropy of the Dixie

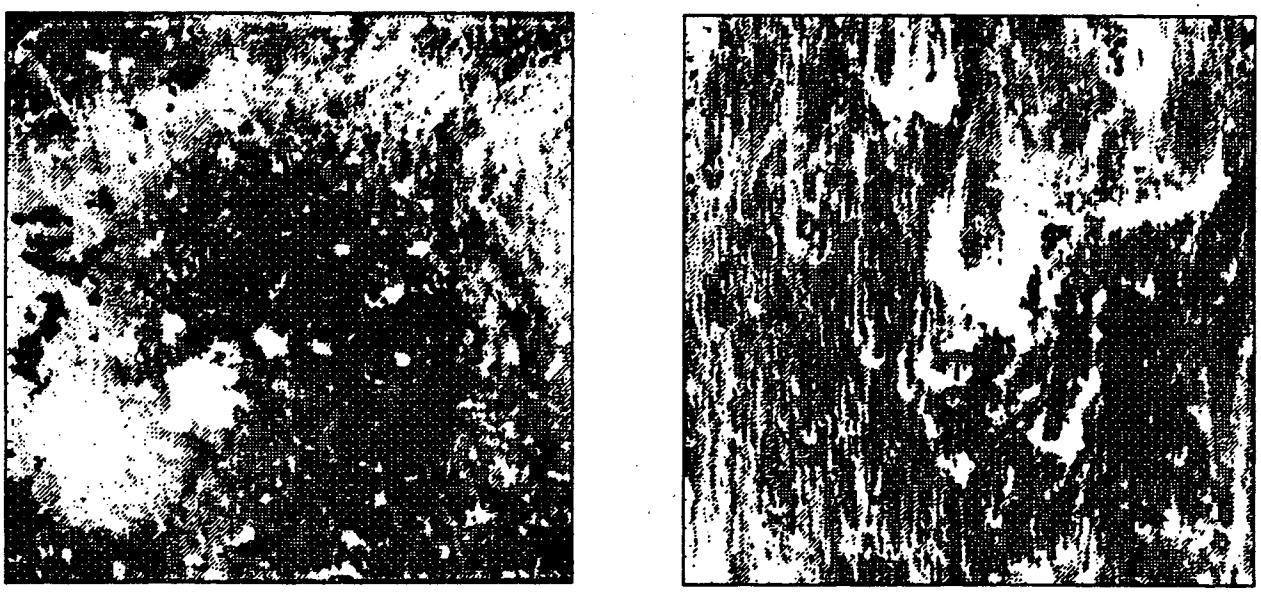

Figure 7. Cutoffs (indicator maps) showing areas of 3 phases for Stripa (a) and Dixie Valley (b) fractures. Black area is rock phase (contact area); grey area is liquid phase; white area is air phase.

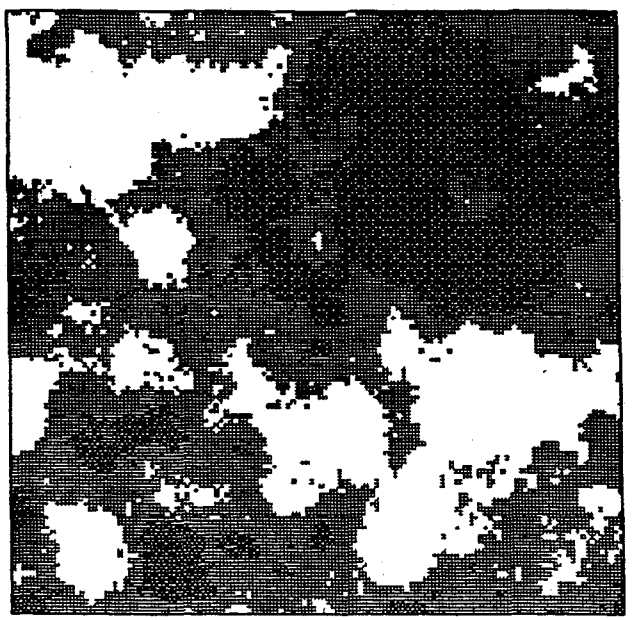

Figure 8. Cutoffs (indicator map) for a simulated aperture with 3 phases. Black area is rock phase (contact area); grey area is liquid phase; white area is air phase.

Valley fracture patterns would be more important for flow properties than the fractal dimension of the total perimeter of the contacts. The fractal dimension is only one piece of information about the pattern geometry and does not indicate connectedness or anisotropy.

ACKNOWLEDGEMENTS

The authors wish to thank Dr. Karsten Pruess and Dr. Yvonne Tsang for reviewing this paper, and Dr. Peter Persoff, for the aperture data sets. Work is performed under the auspices of the Director, Office of Civilian Radioactive Waste Management, Yucca Mountain Site Characterization Project Office, Regulatory and Site Evaluation Division of the U.S. Department of Energy through Contract Number DE-AC03-76SF0098.

REFERENCES

1. W. L. POWER, "Roughness of Natural Fault Surfaces: Implications for Friction and Deformation in Fault Zones," Ph.D. dissertation, Brown University, U.M.I. #9002277, p. 101-141 (1989).

2. B. L. COX, K. PRUESS and P. PERSOFF, "A Casting and Imaging Technique for Determining Void Geometry and Relative Permeability Behavior of a Single Fracture Specimen," Proc. 15th Workshop Geothermal Reservoir Engineering, Stanford University, p. 173-178 (1990).

3. P. PERSOFF and K. PRUESS, "Flow Visualization and Relative Permeability Measurement in a Rough-Walled Fracture," Presented at International High-Level Radioactive Waste Management Conference, Las Vegas, Nevada, April 26-30 (1993) (this volume).

4. P. PERSOFF, K. PRUESS and L. MYER, "Two-Phase Flow Visualization and Relative Permeability Measurement in Transparent Replicas of Rough-Walled Rock Fractures," Presented at the 16th Workshop on Geothermal Reservoir Engineering, Stanford, California, January 23-25 (1991) (LBL-30161).

5. B. B. MANDELBROT, *The Fractal Geometry of Nature*, New York: W. H. Freeman (1982).

6. B. L. COX and J. S. Y. WANG, "Fractal Surfaces: Measurement and Applications in the Earth Sciences," Accepted by *Fractals* (1992) (LBL-31737).

7. B. KLINKENBERG and M. J. GOODCHILD, "The Fractal Properties of Topography: A Comparison of Methods," *Earth Surface Processes and Landforms, 17*, 217-234 (1992).

8. B. B. MANDELBROT, D. E. PASSOJA and A. J. PAULLAY, 1984. "Fractal Character of Fracture Surfaces of Metals," *Nature, 308*, 721-722 (1984).

9. E. H. ISAAKS and R. J. SRIVASTAVA, *An Introduction to Applied Geostatistics*, Oxford University Press, 80-89 (1989).

10. K. PRUESS and Y. W. TSANG, "On Two-Phase Relative Permeability and Capillary Pressure in Rough-Walled Rock Fractures," *Water Resources Research, 26*, (9) 1915-1926 (1990) (LBL-27449).

LAWRENCE BERKELEY LABORATORY
UNIVERSITY OF CALIFORNIA
TECHNICAL INFORMATION DEPARTMENT
BERKELEY, CALIFORNIA 94720